Functional and morphological changes in the testicular tissue of rat newborns during chronic hypoxia (experimental study)

T.V. Palatova*[a], G.N. Maslyakova[a], A.B. Bucharskaya[a], E.A. Genina[b,c], A.N. Bashkatov[b,c]
[a]Saratov State Medical University, 112 B. Kazachaya str., Saratov, Russia, 410012
[b]Research-Educational Institute of Optics and Biophotonics, Saratov State University, 83 Astrakhanskaya str., Saratov, 410012, Russia
[c]Interdisciplinary Laboratory of Biophotonics, Tomsk State University, Tomsk, 36 Lenina Av., 634050, Russia

ABSTRACT

The aim of the study is investigation of morphological features of the testicles of rat newborns with different models of intrauterine hypoxia. Fifteen white outbred female rats aged from 4 to 10 months with a weight of 200 ± 30 g were used. Laboratory animals were divided into 3 experimental groups, 5 rats in each. The first group was subjected to a hypoxic hypoxia during pregnancy (21 days). The hypoxia was simulated in accordance with the method of N.N. Karkishchenko (2010). The second group was subjected to a hemic hypoxia during the second and third weeks of pregnancy, in accordance with the methodology of L.M. Sosedova (2012). The third (control) group was not exposed to any treatment during the pregnancy. After delivery, the newborn rat pups were subjected to the measurements of oxygenation degree using the methods of reflectance spectroscopy, then the animals were withdrawn from the experiment; and a morphological study of the testicle tissues was performed. Histological examination of the tissues of the testicles of newborn rats showed signs of impaired blood circulation, dystrophic and necrobiotic changes in the parenchyma.

Key words: chronic hypoxia, nitrite hypoxia, testicles of newborns, immunohistochemistry, morphology, oxygen saturation

1. INTRODUCTION

Many studies indicate the important role of prenatal hypoxia in the genesis of developmental disorders[1,2]. Prenatal hypoxia has a pathological effect on the functional activity of both individual systems and the whole organism. Antenatal damage to the reproductive system is important, since the consequences can lead to impaired testicular function in the postnatal period and affect fertility potential[3].

The aim of the study is investigation of the morphological features of the testicles of newborns with different models of intrauterine hypoxia.

2. MATERIALS AND METHODS

2.1 Animals

Laboratory animals (white outbred female rats) were divided into 3 experimental groups, 5 females each. The first group underwent hypoxia throughout pregnancy (21 days). Hypoxia modeling was carried out in accordance with the method of N.N. Karkishchenko[4]. The second group underwent hemic hypoxia (nitrite hypoxia) during the second and third week of pregnancy, in accordance with the method of L.M. Sosedova[5]. The third (control) group was not exposed to any effect throughout pregnancy. After delivery, the newborn rat pups were subjected to optical examination, and then the newborn rat pups were removed from the experiment by the cervical dislocation method. The number of pups in the litter was calculated and their body weight was measured. The testicles of male rat pups were taken for morphological studies.

* iamnot88@bk.ru

Saratov Fall Meeting 2019: Optical and Nano-Technologies for Biology and Medicine, edited by Valery V. Tuchin, Elina A. Genina, Proc. of SPIE Vol. 11457, 114570N · © 2020 SPIE
CCC code: 1605-7422/20/$21 · doi: 10.1117/12.2563415

2.2 Morphological study

The testicles of rat pups were fixed in buffered neutral 10% formalin, dehydrated in an alcohol battery of ascending concentration, and embedded in paraffin. Slices of testicular tissue 4–5 μm thick were placed on glass slides and dewaxed according to the accepted standard procedure. Sections were stained with hematoxylin and eosin and used for immunohistochemical staining (IHC). In ten fields of view of each case in the testes, the following indicators were counted: the number of tubules, the number of cells in the tubules, the number of vessels in the stroma, the number of Leydig cells, the diameter of the tubules, the area of the parenchyma and stroma. After dewaxing and rehydration of paraffin sections, an IHG study was performed according to the immunohistochemical staining protocol. The following antibodies were used in the work: Monoclonal Rabbit Anti- Ki67 (1: 100), Monoclonal Mouse anti-Bax (1:50), Polyclonal Antibody to Fibroblast Growth Factor 2 (1:10). Evaluation of immunohistochemical reactions was based on a visual assessment of staining intensity.

2.3 Oxygenation measurement

Newborn rat pups of the first day of life were subjected to oxygen saturation measurement. The experimental studies were performed using a USB4000-Vis-NIR multichannel optical spectrometer with a QR400-7-Vis/NIR fiber-optic probe (Ocean Optics, USA) in the spectral range of 400–1000 nm at room temperature. The fiber-optic probe included six illumination fibers around one receiving fiber. For providing uniform illumination of detection area the probe was placed above skin surface on the distance 2 mm. Five spectra were measured for each animal. A halogen lamp (HL-2000, Ocean Optics, USA) was used as a light source. The spectrometer was calibrated using a WS-1-SL (Labsphere, USA) reflectance standard with a smooth surface.

To exclude the influence of baseline scattering and its changes on the spectra, all obtained were corrected for baseline in the following fashion[6,7]: $D_{corr}\ \lambda = D\ \lambda - a + m\lambda$, were $D\ \lambda = -\log R\ \lambda$ is the apparent optical density measured in course of the experiments, $R(\lambda)$ is the reflectance, λ is the wavelength, $D_{corr}\ \lambda$ is the apparent optical density corrected for the underling scattering, m is the slope of the least squares fitted line to the data between 640 and 820 nm, and a is the intercept of this regression.

For estimation of the oxygen saturation $\left(\mathrm{SatO_2} = \frac{\mathrm{HbO_2}}{\mathrm{HbO_2} + \mathrm{Hb}}\right)$ four different algorithms presented in details in the Refs. [6-12] were used. Here $\mathrm{HbO_2}$ and Hb are the concentrations of oxy- and deoxyhemoglobin, respectively.

Method 1 [8]: $\mathrm{SatO_2} = \alpha\left(\left(\frac{D_{570} - D_{557}}{13} - \frac{D_{557} - D_{545}}{12}\right)\frac{1}{H} + \beta\right)$, where α = 31, β = 1, and $H = \frac{D_{545} - D_{530}}{16} - \frac{D_{570} - D_{545}}{25}$ is the hemoglobin index. Subscripts show corresponding wavelengths.

Method 2 [6, 9]: $\mathrm{SatO_2} = \frac{\mathrm{HbO_2}}{\mathrm{HbO_2} + \mathrm{Hb}}$, where $\mathrm{HbO_2} = \frac{D_{corr}^{574} - D_{corr}^{553} \times K_1}{K_2}$; $\mathrm{Hb} = \frac{D_{corr}^{553} - \mathrm{HbO_2} \times \varepsilon_{oxy}^{553}}{\varepsilon_{deoxy}^{553}}$; $K_1 = \frac{\varepsilon_{deoxy}^{574}}{\varepsilon_{deoxy}^{553}}$; $K_2 = \varepsilon_{oxy}^{574} - \frac{\varepsilon_{oxy}^{553}\varepsilon_{deoxy}^{574}}{\varepsilon_{deoxy}^{553}}$. Superscripts show corresponding wavelengths. $\varepsilon_{oxy}^{\lambda}$ and $\varepsilon_{deoxy}^{\lambda}$ are the molar extinction coefficients for oxy- and deoxyhemoglobin, respectively, at wavelength λ.

Method 3 [10]: $\mathrm{SatO_2} = \frac{\mu_{\mathrm{Hb}}\ \lambda_1 - \mu_{\mathrm{Hb}}\ \lambda_2 \frac{R\ \lambda_2}{R\ \lambda_1}}{\mu_{\mathrm{Hb}}\ \lambda_1 + \mu_{\mathrm{HbO_2}}\ \lambda_1}$, where $R\ \lambda$ is the measured reflectance at the chosen wavelength; λ_1 = 560 nm, λ_2 = 545 nm. μ_{Hb} and $\mu_{\mathrm{HbO_2}}$ are the absorption coefficients of deoxygenated and oxygen-saturated blood, respectively[13].

Method 4 [6, 11, 12]: $\mathrm{SatO_2} = \frac{D_{577} - D_{586} - \frac{9}{17}\ D_{569} - D_{586}}{1.49\ D_{569} - D_{586}} \times 100\%$. Subscripts show corresponding wavelengths.

Method 5 [14, 15]: $\mathrm{SatO_2} = \left[\frac{D_{571.8} - D_{560.1}}{11.7} - \frac{D_{560.1} - D_{548.5}}{11.6} \right] \times \frac{100}{\mathrm{HbI}}$, where $\mathrm{HbI} = \frac{D_{527.1} - D_{500}}{27.1} + \frac{D_{548.5} - D_{527.1}}{21.4} + \frac{D_{548.5} - D_{571.8}}{23.3} + \frac{D_{571.8} - D_{585.4}}{13.6}$. Subscripts show corresponding wavelengths.

Method 6 [16, 17]: $\mathrm{SatO_2} = 150.6 \frac{R\ \lambda = 760\,\mathrm{nm}}{R\ \lambda = 790\,\mathrm{nm}} - 77.41 \cdot$

3. RESULTS AND DISCUSSION

3.1 Morphological study

The number of pups in the litter in the groups did not differ significantly. So, in the first experimental group (hypoxia) the number of newborn rat pups was 27, in the second experimental group (nitrite hypoxia) - 29, and in the control group - 35. The body weight of the offspring also had slight differences (Median 5.8, 5.6 and 6.3 g, respectively). When analyzing morphometric indicators (Table 1), it was found that the diameter of the tubules in the experimental groups was less (Me - 0.043 and 0.026) than in the control group (Me - 0.05). When measuring the area of the parenchyma and stroma, differences in the groups were also revealed. Thus, the area of tubules in the hypoxia groups was less (Me - 0.0111 and 0.0065) compared with the control group (Me - 0.0120). In relation to the stromal component, an inverse relationship was noted. According to the results of the non-parametric Kruskal-Wallis test, significant differences were found between the experimental groups and the control group in the following parameters: tubule diameter ($p < 0.001$), tubule area ($p < 0.001$), stroma area ($p < 0.001$), number of tubules in the field of view ($p < 0.001$), the number of vessels ($p < 0.001$). According to the results of the non-parametric Mann-Whitney test (Table 1), significant differences were also revealed between the experimental groups with different types of hypoxia in the following parameters: tubule diameter ($p < 0.001$), number of tubules ($p < 0.001$), number of vessels ($p < 0.001$), parenchyma area ($p = 0.001$) and stroma area ($p < 0.05$).

An immunohistochemical study of testicular tissue of newborn rat pups showed pronounced expression of the apoptosis marker in both groups, a decrease in the proliferative potential and the absence of expression of fibroblast growth factor in the experimental group. From the literature it is known that the fibroblast growth factor acts as a mitogenic factor, stimulates the proliferation of Sertoli and gonocytes, as well as the production of testosterone and is normally present in all populations of germ cells in the testicle.[18]

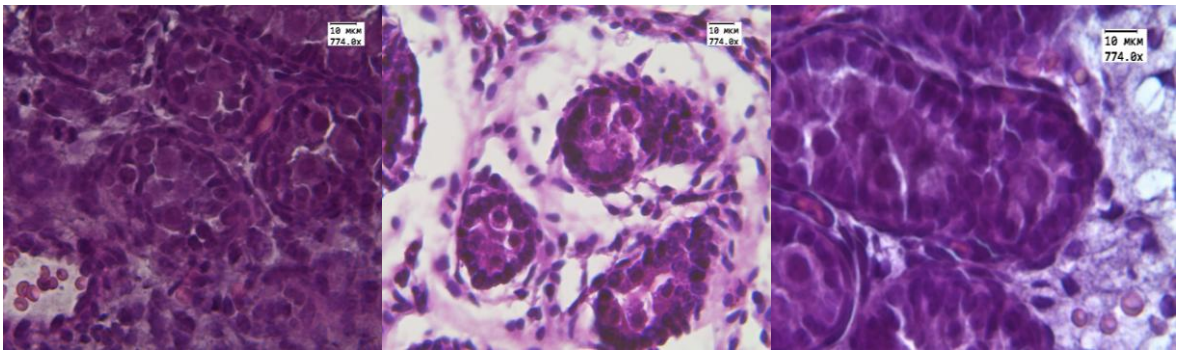

a) b) c)

Figure 1. Testicular tissue. a - testicular tissue of the experimental group (hypoxia). Hematoxylin-eosin, ×774. b - testicular tissue of the experimental group (nitrite hypoxia). Hematoxylin-eosin, ×774. c - testicular tissue of the control group. Hematoxylin-eosin, ×774.

Table 1. Morphometric indicators of the testicles of newborn rats

Quantitative Characteristics	Hypoxic hypoxia group median, [percentiles]	Nitrite hypoxia group median, [percentiles]	Control group median, [percentiles]	*P* level criterion Kraskell-Wallis	*P* level criterion Mann-Whitney
The diameter of the tubules, mm in field of view, ×774	0.043 [0.035;0.046]	0.026 [0.025;0.03]	0.05 [0.046;0.053]	<0.001	<0.001
The number of tubules in field of view, ×774	3 [2;3]	5 [4;6]	4 [3;5]	<0.001	<0.001
The number of cells in the tubules in field of view, ×774	23 [19;27]	23 [19;29]	23 [18;26]	0.061	0/08
Number of vessels in field of view, ×774	4 [3;4]	0.5 [0;1]	2 [1;3]	<0.001	<0.001
Tubular area mm^2 in field of view, ×774	0.0111 [0.0099;0.0116]	0.0065 [0.006;0.0071]	0.012 [0.011;0.013]	<0.001	0.001
Stroma area mm^2 in field of view, ×774	0.0105 [0.01;0.0313]	0.0145 [0.0139;0.015]	0.009 [0.0071;0.01]	<0.001	0.027

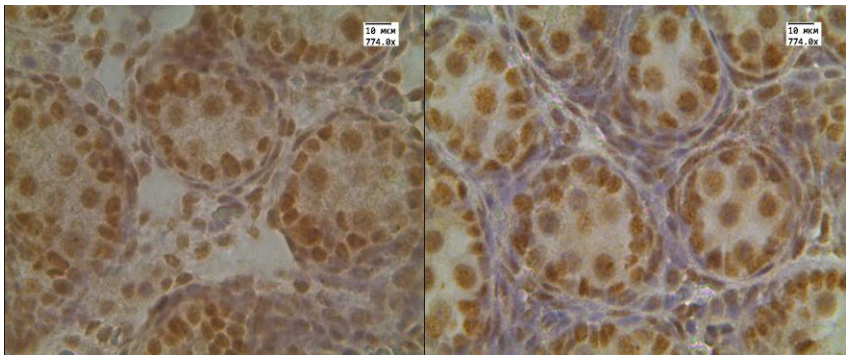

(A) (B)

Figure 2. Testis tissue. A, B - IHC method with a marker of apoptosis (Bax), ×774. A - experimental group, B - control group.

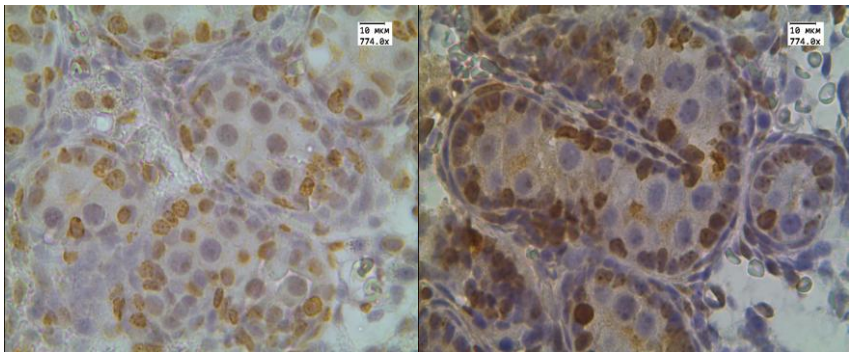

(A) (B)

Figure 3. Testis tissue. A, B - IHC method with a proliferation marker (Ki-67) ×774. A - experimental group, B - control group.

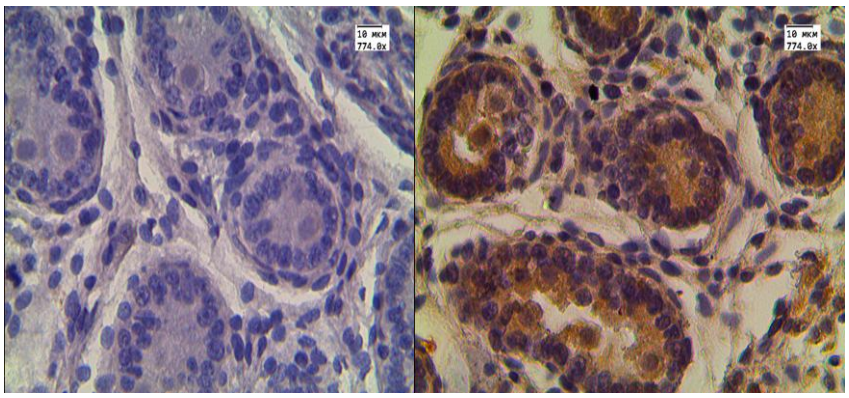

(A) (B)

Figure 4. Testis tissue. IHC method with fibroblast growth factor (FGF 2), ×774. A - experimental group, B - control group.

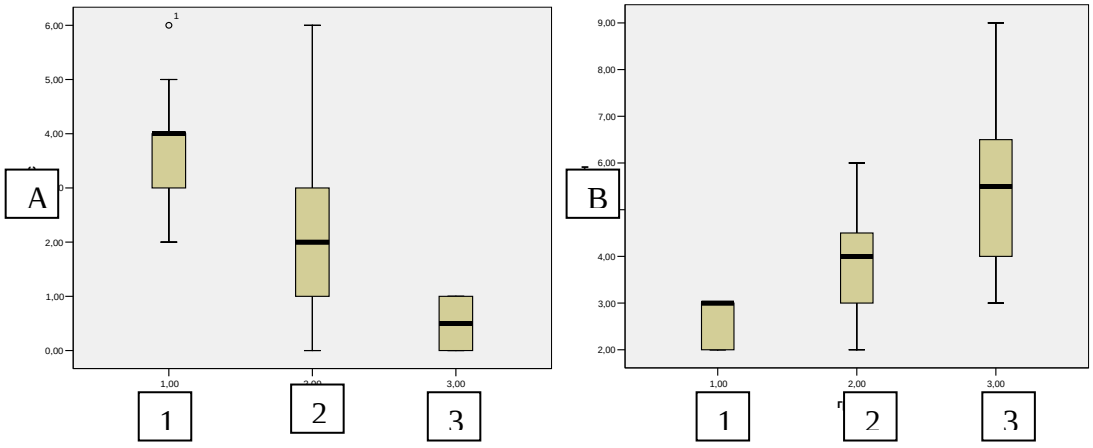

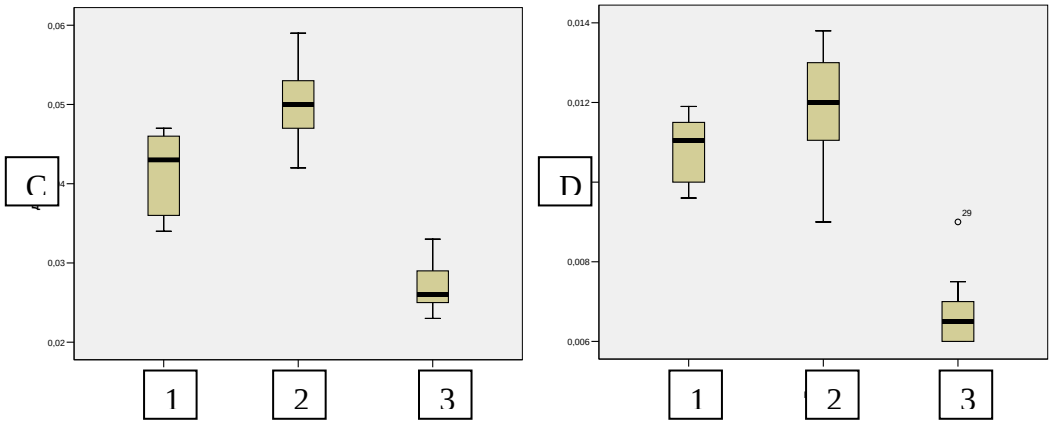

Figure 5. Graphs of the dependence of indicators in groups. A is the number of vessels; B is the number of tubules; C is the diameter of the tubules; D is the area of tubules. 1 - experimental group - hypoxic hypoxia; 2 - experimental group - nitrite hypoxia; 3 - control group.

3.2 Oxygenation measurement

Results of the oxygenation measurements are presented in Tables 2 and 3. Since correction of the experimentally measured reflectance spectra (see, Subsection 2.3) changes the shape of the spectra we have performed calculation of oxygenation degree both with and without the reflectance spectra correction. Mean values of oxygenation degree measured by the six different methods in control group are 35.76±16.02 (immediately after delivery), 39.48±16.01 (two day after delivery), and 30.68±20.12 (seven day after delivery). Mean values of oxygenation degree measured by the six different methods in group with hypoxic hypoxia are 39.9±19.15 (immediately after delivery) and 37.87±17.05 (two day after delivery). Mean values of oxygenation degree measured by the six different methods in group with nitrite hypoxia are 32.57±19.16 (immediately after delivery), 31.12±17.89 (two day after delivery), and 32.34±21.21 (seven day after delivery).

At the same time, comparison of the degree of oxygenation, measured by different methods for the control group and groups with hypoxia, clearly shows that there are no statistically significant differences in the oxygenation degree.

Table 2. The oxygenation degree (%) measured by different methods

Experimental group	Method 1		Method 2		Method 3	
	with spectra correction	without spectra correction	with spectra correction	without spectra correction	with spectra correction	without spectra correction
Control (immediately after delivery)	34.25±16.94	34.32±17.16	43.96±10.84	46.59±1.82	31.86±8.0	26.74±7.2
Control (two day after delivery)	35.06±9.76	35.13±9.88	48.03±7.83	46.88±0.99	31.10±2.83	27.50±2.70
Control (seven day after delivery)	23.42±8.07	23.33±8.17	40.37±7.18	46.43±1.39	29.76±4.77	24.25±4.26
Hypoxic	32.24±12.27	32.26±12.44	51.99±6.93	47.3±0.84	29.31±4.89	25.23±4.85

hypoxia (immediately after delivery)						
Hypoxic hypoxia (two day after delivery)	32.55±11.91	32.60±11.99	49.94±14.06	46.4±3.22	32.81±10.48	27.73±9.96
Nitrite hypoxia (immediately after delivery)	25.36±6.27	25.31±6.35	42.44±4.5	46.5±0.81	31.85±1.72	26.16±2.03
Nitrite hypoxia (two day after delivery)	28.63±6.21	28.62±6.27	36.63±4.75	44.97±1.25	34.26±4.16	29.96±4.89
Nitrite hypoxia (seven day after delivery)	24.48±3.44	24.39±3.47	44.15±4.33	46.78±0.58	28.35±1.8	24.32±2.39

Table 3. The oxygenation degree (%) measured by different methods

Experimental group	Method 4		Method 5		Method 6	
	with spectra correction	without spectra correction	with spectra correction	without spectra correction	with spectra correction	without spectra correction
Control (immediately after delivery)	33.3±13.34	40.02±19.63	19.95±15.65	20.28±15.66	19.95±15.65	77.88±1.84
Control (two day after delivery)	44.36±13.0	61.24±18.11	23.52±7.8	22.68±10.54	24.42±7.88	73.81±7.86
Control (seven day after delivery)	33.97±13.13	47.35±20.14	7.52±7.03	7.97±7.01	7.48±7.04	76.34±1.38
Hypoxic hypoxia (immediately after delivery)	53.6±24.43	69.05±33.83	20.63±11.21	21.14±11.19	20.63±11.21	75.37±0.85
Hypoxic hypoxia (two day after delivery)	47.2±22.28	51.8±28.33	18.93±11.77	19.47±11.63	18.93±11.77	76.04±2.13
Nitrite hypoxia (immediately after delivery)	36.02±9.64	49.71±21.97	10.33±2.9	11.22±2.78	10.33±2.9	75.6±1.07

Nitrite hypoxia (two day after delivery)	28.21±10.87	35.27±7.2	10.83±10.25	9.72±9.56	10.83±10.25	75.48±0.66
Nitrite hypoxia (seven day after delivery)	37.21±3.62	58.22±10.01	7.81±3.35	8.39±3.32	7.81±3.35	76.2±0.79

Our results are consistent with data from several authors, whose studies have demonstrated variability of oxygen saturation (SpO_2) values for neonates of different gestational ages at different time points after birth. SpO_2 values prior to 24 hours are lower and more variable than those seen after 24 hours. Morgan et al.[19] found that mean SpO_2 was 93%–95% within 24 hours among well term neonates. With increasing postnatal age, there is a tendency for increased oxygen saturation, for instance, Ravert et al.[20] found mean SpO_2 of 95%–97% among well term newborns during the first 72 hours. Additional research about oxygenation reference ranges in neonates to select the most optimal research method is needed.

4. CONCLUSION

During intrauterine hypoxia in the testicular tissue of newborn rats, a significant decrease in the number of tubules in the field of view and a decrease in the diameter and area of the tubules with a simultaneous increase in the stroma area were observed; more pronounced changes were observed when rats were exposed to nitrite hypoxia in the antenatal period.

An immunohistochemical study revealed a decrease in proliferative potential and an increase in apoptosis of gonocytes, Leydig and Sertoli cells, as well as a decrease in the expression of fibroblast growth factor, which indicates a delay and impaired development of testicular tissue under hypoxia already in the antenatal period.

ACKNOWLEDGMENTS

The work was supported by the Russian Foundation of Basic Research grant # 18-52-16025.

REFERENCES

[1] Palatova, T.V., Maslyakova, G.N., Bucharskaya, A.B., Medvedeva, A.V., Voronina, E.S., "Morphological characteristics of fetal testes in chronic intrauterine hypoxia in different gestation periods," Archive of Pathology 4(80), 21-26 (2018). DOI: 10.17116/patol201880421

[2] Reyes, J.G., Farias, J.G., Henríquez-Olavarrieta S., "The Hypoxic Testicle: Physiology and Pathophysiology // Oxidative Medicine and Cellular Longevity," 2012. 15 pages. https://dx.doi.org/10.1155/2012/929285

[3] Palatova, T.V., Bucharskaya, A.B., Medvedeva, A.V., Voronina, E.S., Maslyakova, G.N., "Influence of chronic intrauterine hypoxia on development of testicles of newborns," Russian Open Medical Journal 7(2), 1-5 (2018).

[4] Karkishchenko, N.N., Grachev, S.V., [Manual on laboratory animals and alternative models in biomedical technologies], Moscow, Russia: Profile, 358 (2010).

[5] Sosedova L.M., Vokina V.A., Rukavishnikov V.S., Patent RU No. 2497202. Method for simulating prenatal hypoxic encephalopathy in small laboratory animals. Bull. No. 30. Published October 27, 2013.

[6] Gade, J., Palmqvist, D., Plomgard, P., Greisen, G., "Diffuse reflectance spectrophotometry with visible light: comparison of four different methods in a tissue phantom," Phys. Med. Biol. 51, 121-136 (2006).

[7] Knoefel, W.T., Kollias, N., Rattner, D.W., Nishioka, N.S., Warshaw, A.L., "Reflectance spectroscopy of pancreatic microcirculation," J. Appl. Physiol. 80(1), 116-123 (1996).

[8] Nakhaeva, I.A., Mohammed, R.M., Zyuryukina, O.A., Sinichkin, Yu.P., "The effect of an external mechanical compression on in vivo optical properties of human skin." Opt. Spectrosc. 117(3), 506-512 (2014).
[9] Knoefel, W.T., Kollias, N., Warshaw, A.L., Waldner, H., Nishioka, N.S., Rattner, D.U., "Pancreatic microcirculatory changes in experimental pancreatitis of graded gravity in rats," Surgery 116, 904-963 (1994).
[10] Potapova, E.V., Dremin, V.V., Zherebtsov, E.A., Makovik, I.N., Zherebtsova, A.I., Dunaev, A.V., Podmasteryev, K.V., Sidorov, V.V., Krupatkin, A.I., Khakhicheva, L.S., Muradyan, V.F., "Evaluation pf microcirculatory disturbances in patients with rheumatic diseases by the method of diffuse reflectance spectroscopy," Human Physiology 42(2), 222-228 (2017).
[11] Sato, N., Matsumura, T., Shichiri, M., Kamada, T., Abe, H., and Hagihara, B., "Hemoperfusion, rate of oxygen consumption and redox levels of mitochondrial cytochrome c (+c1) in liver in situ of anesthetized rat measured by reflectance spectrophotometry," Biochim. Biophys. Acta 634(1), 1-10 (1981).
[12] Kinuta, Y., Kikuchi, H., Ishikawa, M., Hirai, O., Imataka, K., Kobayashi, S., "Reflectance spectrophotometric measurement of in vivo local oxygen consumption in the cerebral cortex," Journal of Cerebral Blood Flow and Metabolism 7(5), 592-598 (1987).
[13] Bosschaart, N., Edelman, G.J., Aalders, M.C.G., van Leeuwen, T.G., Faber, D.J., "A literature review and novel theoretical approach on the optical properties of whole blood," Lasers Med. Sci. 29, 453-479 (2014).
[14] Harrison, D.K., Evans, S.D., Abbot, N.C., Beck, J.S., McCollum, P.T., "Spectrophotometric measurements of haemoglobin saturation and concentration in skin during the tuberculin reaction in normal human subjects," Clin. Phys. Physiol. Meas. 13(4), 349-363 (1992).
[15] Nasseri, N., Kleiser, S., Wolf, U., Wolf, M., "Tissue oximetry reflective visible light spectroscopy: comparison of algorithms and their robustness," J. Biophotonics 11(9), e201700367 (2018).
[16] Sircan-Kucuksayan, A., Uyuklu, M., Canpolat, M., "Diffuse reflectance spectroscopy for the measurement of tissue oxygen saturation," Physiol. Meas. 36(12), 2461-2469 (2015).
[17] Can, O.M., Ulgen, Y., "Estimation of free hemoglobin concentrations in blood bags by diffuse reflectance spectroscopy," J. Biomed. Opt. 23(12), 127001 (2018).
[18] Jiang, X., Skibba, M., Zhang, C., Tan, Y., Xin, Y., Qu, Y., "The Roles of Fibroblast Growth Factors in the Testicular Development and Tumor," Journal of Diabetes Research 2013, 489095 (2013). DOI: 10.1155/2013/489095
[19] Morgan, M.C., Maina, B., Waiyego, M., Mutinda, C., Aluvaala, J., Maina, M., English, M., "Oxygen saturation ranges for healthy newborns within 24 hours at 1800 m," Arch. Dis. Child Fetal Neonatal Ed. 102, F266–F268 (2017).
[20] Ravert, P., Detwiler, T.L., Dickinson, J.K., "Mean oxygen saturation in well neonates at altitudes between 4498 and 8150 feet," Adv. Neonatal Care 11, 412–417 (2011).